

## Direct patterning of surface quantum wells with an atomic force microscope

J. Cortes Rosa, M. Wendel, H. Lorenz,<sup>a)</sup> and J. P. Kotthaus  
*Sektion Physik, Ludwig-Maximilians-Universität München, D-80539 München, Germany*

M. Thomas and H. Kroemer  
*Department of Electrical and Computer Engineering, University of California, Santa Barbara, California 93106*

(Received 15 July 1998; accepted for publication 8 September 1998)

We employ an atomic force microscope to directly pattern the electron system of InAs–AlSb surface quantum wells. Sharp and sturdy electron beam deposited tips are developed to withstand the comparatively high ( $\approx \mu\text{N}$ ) forces in the direct patterning process. By direct patterning the InAs surface quantum well we modulate the electron system without any mask. We are therefore able to directly transfer the excellent lithographic resolution of atomic force microscopy to an electron system. The magnetoresistance of such fabricated antidot arrays is discussed. © 1998 American Institute of Physics. [S0003-6951(98)04744-5]

Both lithographic resolution as well as pattern transfer techniques limit the smallest electronically active feature sizes that presently can be defined in semiconductor devices. To overcome existing lithographic limitations in, e.g., electron beam lithography, new scanning probe techniques have been developed during the last years. Here atomic force microscope (AFM) lithography is particularly promising as an AFM is not restricted to conducting materials.<sup>1</sup> Parallel to the shrinking of the lithographically defined mask features, the transfer process of the mask pattern to the electron system becomes increasingly critical. The precision of the most common transfer mechanisms—etching and gating—is diminished as the distance between the electron system and the surface increases.<sup>2</sup> In GaAs–AlGaAs heterojunctions, a favorite material in research on low dimensional electron systems, one has in addition lateral electronic depletion caused by surface-induced band bending which is of the same order as the distance to the surface of typically 50–100 nm.

To overcome the limitations in feature definition caused by conventional pattern transfer and surface depletion, we employ here direct patterning of an InAs surface quantum well. We use the vibrating AFM tip to mechanically modify the surface quantum well directly with an estimated force of several  $\mu\text{N}$ .<sup>3</sup> InAs surface quantum wells are chosen since, in contrast to GaAs–AlGaAs heterojunctions, there is no noticeable surface depletion in InAs. Recently a similar method for direct patterning of III–V semiconductors has been reported.<sup>4</sup> In contrast to this publication we do not use the patterned semiconductor surface layer as an etch mask but rather directly pattern a structure on the two-dimensional electron system.

The layer sequence of the quantum well used is schematically plotted in Fig. 1 and has three main advantages for the size reduction in electronic systems. First, the quantum well contains the two-dimensional electron system (2DES) immediately at the surface. The etch depth, necessary to re-

move the electron system is only a few nanometers, thus enabling the creation of very small patterns even with isotropic etchants. Second, InAs is a comparatively soft semiconductor material. The forces, necessary to pattern the surface layer, are significantly smaller than in silicon or GaAs. This allows a reliable direct modification of the InAs surface with the AFM tip. It is not necessary to modify a mask material and to transfer the lithographic pattern afterwards into the electron system. Furthermore, since there is no concomitant broadening process as, e.g., through an isotropic etch step, the smallest feature size is limited only by the AFM tip and the direct patterning mechanism. For comparison, however, we also patterned thin spin-coated photoresist films covering the surface by AFM lithography and transferred the patterns to the electron system by wet chemical etching in  $\text{H}_2\text{O}:\text{CH}_3\text{COOH}:\text{H}_2\text{O}_2=50:5:1$ . This isotropic acid selectively etches the InAs top layer and stops at the AlSb layer below. The third advantage of the quantum well system employed is the absence of lateral depletion zones in InAs since there is no pinning of the Fermi level in the band gap of

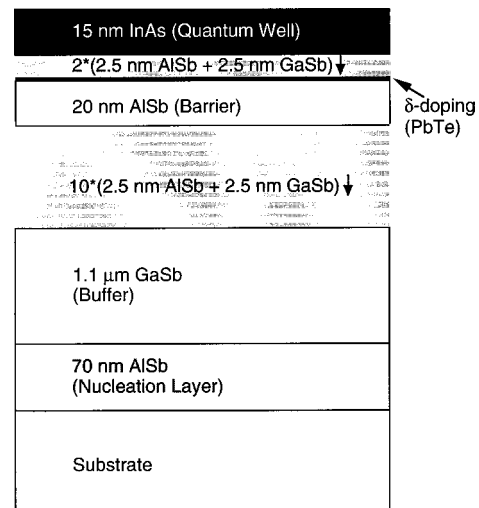


FIG. 1. Layer sequence of the InAs–AlSb surface quantum well.

<sup>a)</sup>Electronic mail: bert.lorenz@physik.uni-muenchen.de

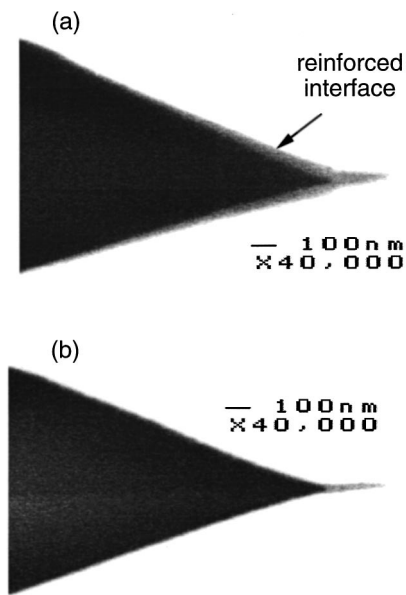


FIG. 2. Electron beam deposited tip with reinforced interface to the silicon (arrow) used for lithography. The electron micrographs have been taken before (a) and after the sharpening process (b).

InAs.<sup>5</sup> In contrast to GaAs–AlGaAs heterojunctions with a typical depletion length of 50–100 nm,<sup>6</sup> the topography of surface patterns rather directly reflects the electron density in this material system. This allows us to transfer the excellent lithographic resolution of AFM lithography to an electronic modulation.

In spite of InAs being much softer than Si or GaAs, the lithographic force needed for direct patterning is still 2–3 times larger than in photoresist. Therefore there are rather stringent requirements to the mechanical stability and durability of the tips. We employ sharpened electron beam deposited (EBD) tips. The fabrication and sharpening procedures as well as the material properties are published elsewhere.<sup>7,8</sup> EBD tips are extremely sharp and robust and do not blunt significantly during the lithographic step. At forces well above several  $\mu\text{N}$ , however, the tip can break off at the interface to the silicon substrate. To prevent this, we now reinforce this interface by coating the underlying silicon material with a thin (about 50–100 nm) layer of EBD material immediately before growing the tip. Figure 2 depicts a tip before and after the sharpening process. In the electron micrograph the EBD layer appears brighter and can easily be distinguished from the silicon. Such improved tips stand a significant higher force before breaking and allow a very reliable and high resolution AFM lithography.

The AFM micrographs in Fig. 3 depict three hole arrays fabricated into InAs surface quantum wells. The upper micrograph [Fig. 3(a)] shows two antidot arrays, transferred into a hall bar mesa by wet chemical etching. The hole periods of the arrays are 98 and 85 nm, respectively, with the hole diameter 40–50 nm and the depth about 15 nm. The holes thus penetrate to the bottom of the 15-nm-thick quantum well. Figure 3(b) depicts an array of directly patterned holes with a period of 55 nm, fabricated into a 8 nm thin quantum well. The array was scanned with the same tip that fabricated the structure immediately after the lithography,

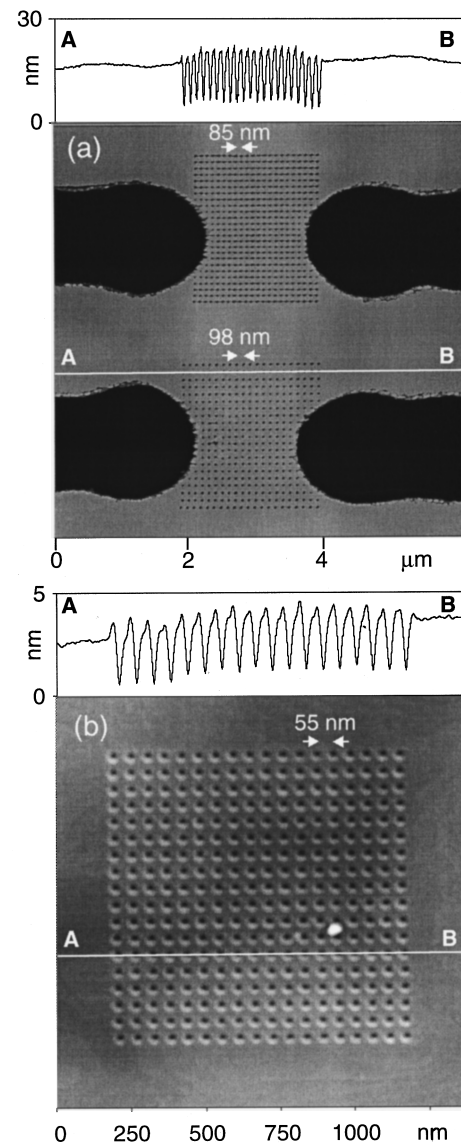


FIG. 3. Periodic hole arrays in an InAs–AlSb surface quantum well, fabricated by selective wet etching through a photoresist mask (a) and by direct lithography of the InAs top layer (b). The hole period of the wet etched arrays is 98 nm (bottom) and 85 nm (top), the period of the direct structured array is 55 nm. The mesa depth of the left sample is about 70 nm. Top of the micrographs: Section plots along the indicated lines. The AFM micrographs are taken with sharpened EBD tips.

detecting a hole depth of about 3 nm. However, the AFM tips possibly may not reach the bottom of these very tiny holes and therefore the hole depth might be slightly larger. Nevertheless the holes probably do not reach to the bottom of the quantum well and so they might only cause an electron density modulation but no complete electron depletion. In the line scan of the micrograph Fig. 3(b) one additionally detects small walls around the holes which are created by removed InAs during the lithographic step. The directly patterned holes have a diameter of only a few nanometers and therefore are much smaller than the wet etched holes with a diameter of about 40–50 nm. The direct patterning of the surface quantum well significantly increases the lithographic resolution.

In our experiments we use a nominally 15-nm-thick InAs–AlSb based surface quantum well with the 2DES lo-

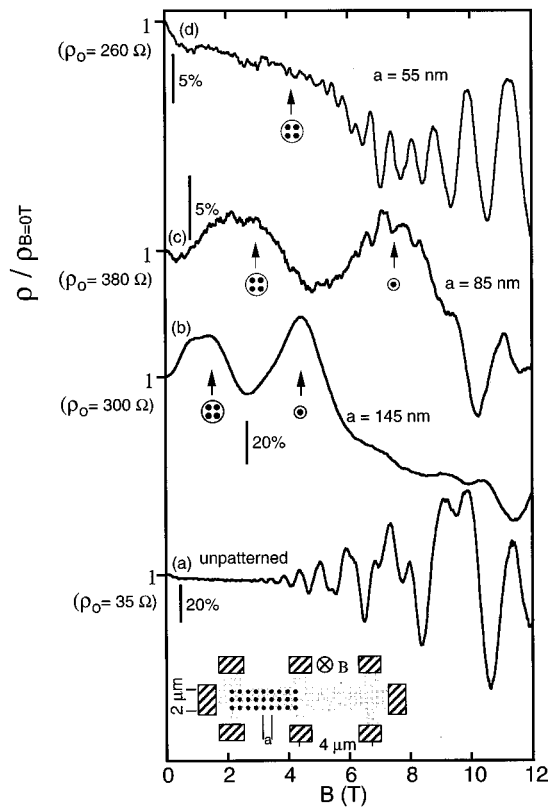


FIG. 4. Normalized magnetoresistivity at temperature  $T=4.2$  K of the unstructured InAs–AlSb surface quantum well (a), wet chemically defined antidot arrays with a period of 145 nm (b), and directly written hole arrays with periods of 85 nm [(c), hole depth 6 nm] and 55 nm [(d), hole depth 3 nm]. The arrows mark magnetic fields where commensurability oscillations are expected. The inset depicts the sample geometry.

cated within the InAs surface layer. Whereas in earlier publications growth parameters and optical properties of InAs-based surface quantum wells have been of interest,<sup>9–11</sup> we here report on transport properties of InAs–AlSb surface quantum wells, patterned by high resolution AFM lithography. The antidots are fabricated into hall bar devices with widths varying from 1.5 to 2.5  $\mu\text{m}$  and distances between the voltage probes from 3 to 5  $\mu\text{m}$ . All data were taken on 15-nm-thick quantum wells, except for the samples with a period of 55 nm. Here the quantum well thickness is about 8 nm.

Typical magnetoresistance data, measured at a temperature of  $T=4.2$  K are shown in Fig. 4. While the magnetoresistance of the unpatterned sample segment exhibits only Shubnikov–de Haas oscillations [curve (a)], additional maxima in the resistance of wet etched antidot arrays [curve (b) (antidot period  $a=145$  nm)] dominate the low field magnetoresistance. These so-called commensurability oscillations are typical for antidot devices and already have been studied in detail by many authors in GaAs–AlGaAs heterostructures.<sup>12</sup> Investigations of AFM-defined antidot arrays in GaAs–AlGaAs heterostructures are published elsewhere.<sup>13</sup> The commensurability oscillations can be seen at magnetic fields where the cyclotron orbit fits well in the hole array, as indicated in Fig. 4. In the sample with the period  $a=55$  nm the maximum concerning the orbit around one antidot is expected at a magnetic field of  $B>12$  T and thus is not seen.

The magnetoresistance of directly patterned hole arrays with periods of 85 and 55 nm, respectively, is depicted in curves c and d in Fig. 4. The corresponding hole depth is 6 and 3 nm, respectively, the hole diameter is only a few nanometers. While the 6 nm deep holes still exhibit clear commensurability oscillations, the amplitude of the maxima decreases at the 3 nm deep holes. However, the zero field resistance is still an order of magnitude larger as compared to the unpatterned sample segment. As hole depth and diameter are smaller than in wet etched samples, the resistivity at  $B=0$  T is significantly smaller than in wet etched arrays with the same period. This indicates that the action of the direct patterning on the electron system is restricted essentially to the hole area visible in topography.

In summary we demonstrated a very suitable maskless lithographic technique to pattern an InAs–AlSb surface quantum well with extremely robust and sharp tips of an atomic force microscope. Because of the absence of lateral depletion lengths of this material system the topographic changes directly reflect the electronic density. Therefore we now are able to transfer the excellent resolution of the lithographic technique to an electronic modulation. The density variation can be altered by the topographic depth and therefore by the lithographic force. Hole arrays with periods as small as 26 nm such have been fabricated. Magnetotransport data of such fabricated antidot arrays are discussed.

The authors would like to thank B. Irmer and A. Kriele for excellent collaboration and M. Hartung, A. Lorke, and A. Wixforth for fruitful discussions. The work in Munich was sponsored by the Volkswagen-Stiftung. The Santa Barbara group gratefully acknowledges support through QUEST, the National Science Foundation Science and Technology Centre for Quantized Electronic Structures (Grant No. DMR 91-20007). The international collaboration was also supported by the BMBF via a Max Planck Research Award.

<sup>1</sup>O. T. Teuschler, K. Mahr, S. Miyazaki, M. Hundhausen, and L. Ley, Appl. Phys. Lett. **66**, 2499 (1995), and references given therein.

<sup>2</sup>J. P. Kotthaus and D. Heitmann, Surf. Sci. **113**, 481 (1982).

<sup>3</sup>M. Wendel, S. Kühn, H. Lorenz, J. P. Kotthaus, and M. Holland, Appl. Phys. Lett. **65**, 1775 (1994).

<sup>4</sup>R. Magno and B. R. Bennett, Appl. Phys. Lett. **70**, 1855 (1997).

<sup>5</sup>See, e.g., L. O. Olsson, C. B. M. Andersson, M. C. Hakansson, J. Kanski, L. Ilver, and U. O. Karlsson, Phys. Rev. Lett. **76**, 3626 (1996); S. Bhargava, H.-R. Blank, V. Narayanamurti, and H. Kroemer, Appl. Phys. Lett. **70**, 759 (1997).

<sup>6</sup>K. K. Choi, D. C. Tsui, and K. Alavi, Appl. Phys. Lett. **50**, 110 (1986).

<sup>7</sup>M. Wendel, H. Lorenz, and J. P. Kotthaus, Appl. Phys. Lett. **67**, 3732 (1995).

<sup>8</sup>M. Wendel, B. Irmer, J. Cortes, H. Lorenz, J. P. Kotthaus, A. Lorke, and E. Williams, Superlattices Microstruct. **20**, 349 (1996).

<sup>9</sup>C. Nguyen, B. Brar, H. Kroemer, and J. English, J. Vac. Sci. Technol. A **10**, 898 (1992).

<sup>10</sup>J. Dreybrodt, A. Forchel, and J. P. Reithmaier, Phys. Rev. B **48**, 14741 (1993).

<sup>11</sup>R. Steffen, Th. Koch, J. Oshinowo, and A. Forchel, Appl. Phys. Lett. **68**, 223 (1996).

<sup>12</sup>See, e.g., D. Weiss, M. L. Roukes, A. Menschig, P. Grambow, K. von Klitzing, and G. Weimann, Phys. Rev. Lett. **66**, 2790 (1991); R. Schuster, K. Ensslin, J. P. Kotthaus, M. Holland, and C. Stanley, Phys. Rev. B **47**, 6843 (1993).

<sup>13</sup>R. Kaiser, B. Irmer, M. Wendel, T. Schlösser, H. Lorenz, A. Lorke, K. Ensslin, J. P. Kotthaus, and A. C. Gossard, in *The Physics of Semiconductors* edited by M. Scheffler and R. Zimmermann (World Scientific, Singapore, 1996), Vol. 2, p. 1501, and references given therein.